Artificial Intelligence for Mitigation Against Array Perturbations in Direction of Arrival Estimation

Thesis Defense

Mathew Shaham

Electrical Engineering Department
Cal Poly San Luis Obispo

Thesis Defense

Table of Contents

Table of Contents

Problem Statement

- Super-resolution Direction of Arrival (DOA) algorithms rely on known array geometry. What if this is not known?
- Can DOA still be determined from received signal using a neural network approach?
- What are some of the limitations in using a neural network?

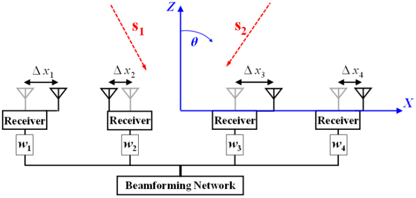

Figure: Array Element Perturbations

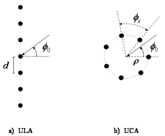

Figure: ULA & UCA Array Configuration [1]

Big Picture

- Search & Rescue Application: Minimal Sensors
- ARDC Project: "Direction Finding from Aerial Platforms with Amateur Radio Digital Arrays"
- Ground Station for digital beamformer (DBF) processing.

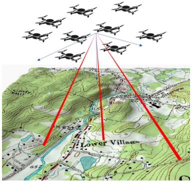

Figure: UAV Swarm for DOA Estimation

Ranging

Determining distances between multiple UAV platforms

Synchronization

Ensuring received signals can be sent after synchronizing transceivers on each UAV platform

Hardware

Low altitude balloon with single board computer and transceiver

Alternative DOA Estimation Techniques

Alternatives to classical DOA methods for unique scenarios with limited resources

Digital Beamforming

- Digital Beamformers have entire RF receive (RX) chains and are combined at baseband
- This yields N channels of RX signals that can be used for processing

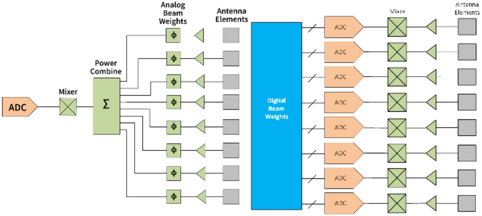

Figure: Left: Analog Beamformer, Right: Digitalbeamformer (DBF) [2]

Previous Work Comparison

- Less quantifiable method of general perturbations
- Extensive previous work for DOA estimation of correlated signals

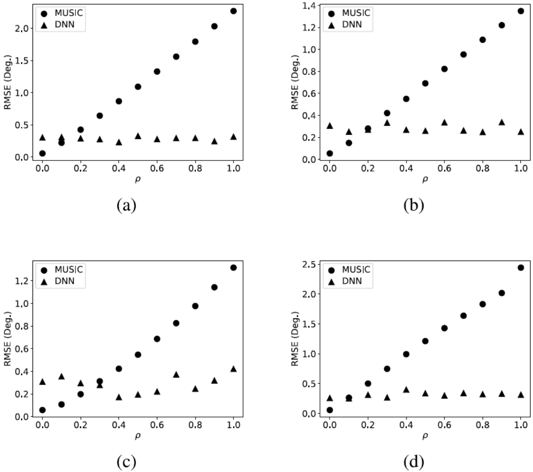

Figure: (a) Gain & Phase Imperfections (b) Sensor Position Error (c) Mutual Coupling (d) Combined Imperfection [3]

Table of Contents

Model Assumptions

Assumption 1

Non-Coherent (Non-Correlated) Signal Sources

Assumption 2

Wide Sense Stationary (WSS): Constant Mean & Covariance only time difference dependent

Assumption 3

Isotropic Antenna Elements

Assumption 4

Additive White Gaussian Noise (AWGN) added to received signal at each array element

Classical Arrays

- Resolution Limited by Rayleigh Limit: $\frac{FNBW}{2}$
- DOA estimation with main beam has many limitations
- $E(\theta)_{dB} = 20 * log_{10}[\frac{sin(\frac{N}{2}\psi)}{sin(\frac{1}{2}\psi)}]$

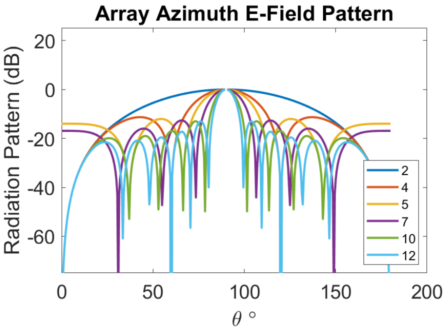

Figure: Array azimuth pattern for different number of elements in array

Array Steering Vector (ASV) & Sample Covariance Matrix

- Array Steering Vector:
$x = \sum_{m=1}^{M} \sum_{n=1}^{N} w_n(s_m e^{jk(n-1)dsin\theta_m} + v_n) = \mathbf{w}(\mathbf{A}\mathbf{s}^{\mathbf{T}} + \mathbf{N})$

$$\begin{bmatrix} 1 & 1 & \cdots & 1 \\ e^{jkdsin\theta_1} & e^{jkdsin\theta_2} & \cdots & e^{jkdsin\theta_M} \\ \vdots & \vdots & \ddots & \vdots \\ e^{jk(N-1)dsin\theta_1} & e^{jk(N-1)dsin\theta_2} & \cdots & e^{jk(N-1)dsin\theta_M} \end{bmatrix}$$

- Sample Covariance Matrix (SCM) for K Signal Snapshots:

$$R_{ss} = \frac{s * s^H}{K}, R_{nn} = \frac{n * n^H}{K}, R_{ns} = \frac{n * s^H}{K}, R_{sn} = \frac{s * n^H}{K}$$

- Linear Combination: $\hat{R_{rr}} = A * R_{ss} * A^H + A * R_{sn} + R_{ns} * A^H + R_{nn}$
- In practice the SCM is: $\hat{R_{rr}} = \frac{1}{K}[x * x^H]$

Eigenbeamforming

- Eigenvalue Decomposition (EVD) of the Covariance Matrix yields Noise and Signal Eigenvalues and Eigenvectors represented by Λ and U respectively in $U \Lambda U^H$.
- Noise eigenvalues are N-M smallest values. The signal and noise subspaces are orthogonal: U=$[U_S U_N] \rightarrow U_S \perp U_N$.
- If the number of signals (M) is known, then the corresponding column of Eigenvectors based on the largest M Eigenvalues can be used as the new array weights.

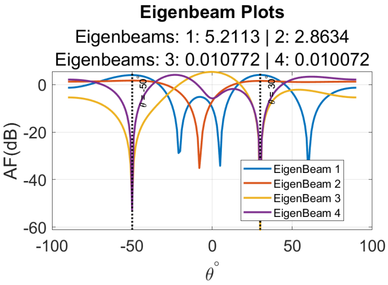

Figure: Eigenbeamformer Example 2 Signals

Multiple Signal Classification (MUSIC)

- Subspace-based method that creates a pseudo-spectrum based on given resolution by inverting the noise eigenvectors.
- Take the minimum noise eigenvalue & corresponding eigenvectors. Create an ASV from a pseudo-spectrum of some angular resolution for chosen range.
- $P_{MUSIC} = 20 * log_{10}(\frac{1}{|A(\theta)^H * U_N|^2})$

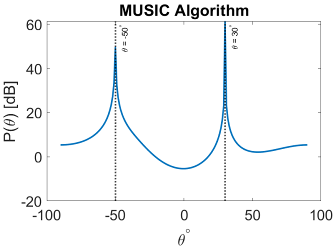

Figure: MUSIC with 2 Signals for 1° Resolution

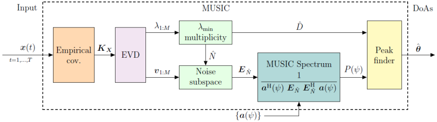

Figure: Summary of MUSIC Process [4]

MUSIC and Number of Signal Snapshots

- More signal snapshots yields a more accurate sample covariance matrix
- False peaks increased, main peak power reduced

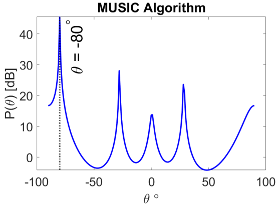

Figure: MUSIC with a single -80° source with 100 Snapshots

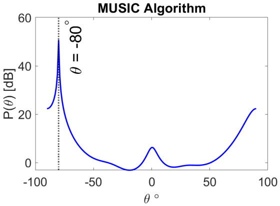

Figure: MUSIC with a single -80° source with 5000 Snapshots

Estimation of Signal Parameters using Rotational Invariance Techniques (ESPRIT)

- Only outputs DOA estimate, can distinguish correlated signals, uses 2 sub-arrays
- ESPRIT takes 2 Eigenvalue Decomposition (EVD) to compute the DOA estimate
- EVD of the overall Sample Covariance Matrix taken. Sub-arrays formed by taking 1:N-1 and 2:N columns of the eigenvectors
- Take the Q_S largest M eigenvectors for each sub-array, then form Ψ by taking the ratio of the eigenvectors from each sub-array
- To determine Ψ the Pseudo Inverse is taken: $\Psi = (Q_0^H * Q_0)^{-1} * Q_0^H * Q_1$
- Using this the DOA can be determined by taking the inverse tangent of complex value Ψ and the inverse sine will be the angle in θ angular space

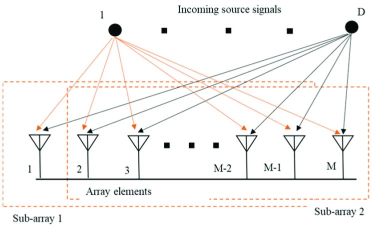

Figure: Sub-arrays and representation of plane wave signals [5]

Table of Contents

Neural Network (NN) Background (1)

- NNs allow nonlinear mapping between problem and solution spaces
- The Convolution Operation determines weights applied to the input (feature maps) that work alongside neurons in the fully connected layers to provide correct output
- Regression & Classification Networks are most common with Regression uses Mean Squared Error (MSE) Loss Functions, whereas Classification Networks have categorical cross-entropy losses

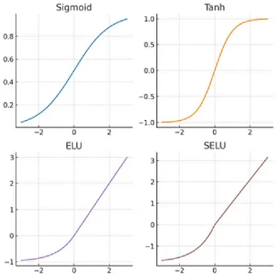

Figure: Examples of Some Activation Functions [6]

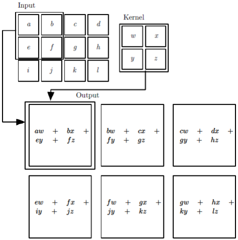

Figure: Convolution Operation Example [7]

NN Background (2)

- Bias-Variance Tradeoff: Ensuring data is varied over the problem space and network is sufficiently complex
- Dropout during training can help overfitting and generalization, but degrade performance for too large probability.
- Reduce internal covariate shift with Batch Normalization & improve convergence
- Backpropagation & Optimization Methods

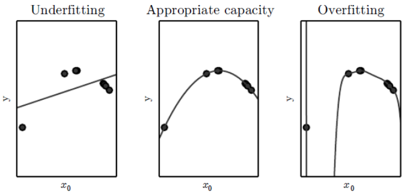

Figure: Underfitting, Appropriate Complexity, and Overfitting [7]

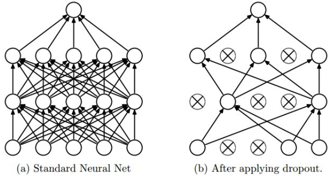

Figure: Dropout in Fully Connected Layers (During Training) [8]

Previous Work (1)

- Deep AoANet: Fully Connected Network has 4.86M parameters, whereas the CNN has 2.86M parameters
- Field of View: $\pm 37°$ with $2°$ resolution the Mean Absolute Error (MAE) for FC Network: $2.101°$ and the MAE for the CNN: $1.954°$
- Input data set used vertical concatenation: b=[Real;Imag] and normalized the data before using it for training: $\frac{b}{||b||}$

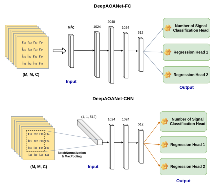

Figure: Deep AOANet 2 Network Topologies [9]

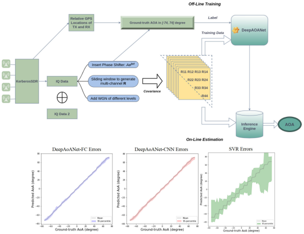

Figure: Creating Training Samples and Network Performance Deep AOANet [9]

Previous Work (2)

- Deep MUSIC Parallel CNN for Subregion Classifications
- Deep Augmented (DA) MUSIC implementation.

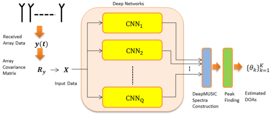

Figure: Deep MUSIC Parallel CNNs [10]

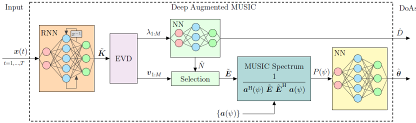

Figure: Deep-Augmented (DA) MUSIC Topology with RNN used in place of sample covariance matrices [4]

- Convolutional Autoencoder (CAE): Squeezes input down to small size and attempts to reconstruct original input, determining features
- Root-MUSIC is polynomial based, thus inherently differentiable

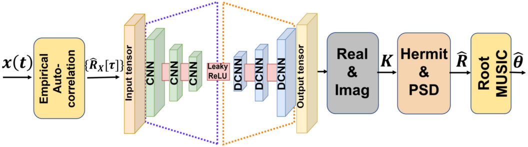

Figure: Deep Root MUSIC Network Topology [11]

Table of Contents

Effect of Element Perturbations on Classical DOA (1)

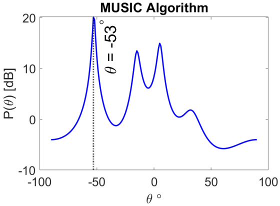

Figure: 0.1λ Average Perturbation Multiplier 1000 Snapshots -50° Single Source

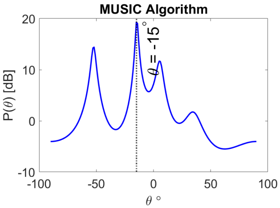

Figure: 0.15λ Average Perturbation Multiplier 1000 Snapshots -50° Single Source

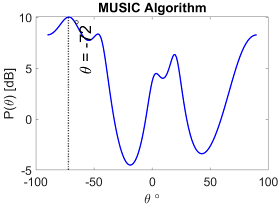

Figure: 0.1λ Average Perturbation Multiplier 5000 Snapshots

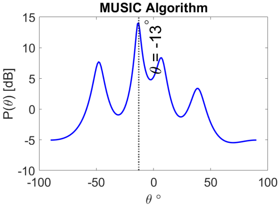

Figure: 0.25λ Average Perturbation Multiplier 1000 Snapshots -50° Single Source

Effect of Element Perturbations on Classical DOA(2)

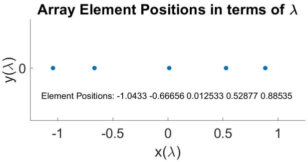

Figure: Element positions under random perturbations with average perturbation 0.1λ for the ULA with initial spacing $\frac{\lambda}{2}$

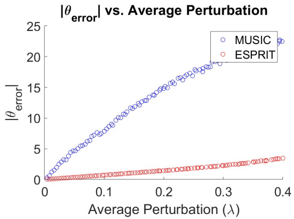

Figure: Absolute angular error from DOA estimate for 100 average perturbation multipliers averaged over 5,000 samples for each average perturbation for single source DOA: 10°

Effect of Element Perturbations on Classical DOA(3)

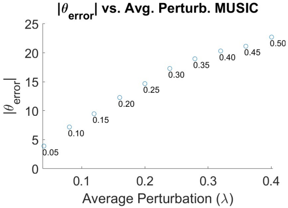

Figure: 10 Average Perturbation value for MUSIC averaged over 5000 samples for a given perturbation multiplier

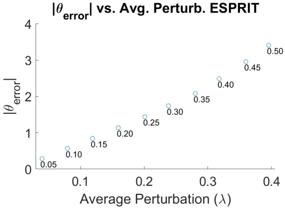

Figure: 10 Average Perturbation value for ESPRIT averaged over 5000 samples for a given perturbation multiplier

Effect of Element Perturbations on Classical DOA(4)

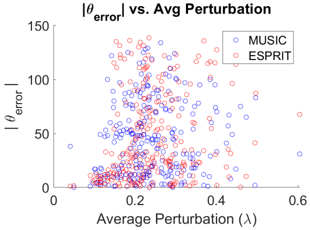

Figure: Single Source 50° with 50 Samples Per Average Perturbation Multiplier from 0.1λ in 0.1 increments for 1000 Snapshots for 0.1λ:0.1:0.5λ

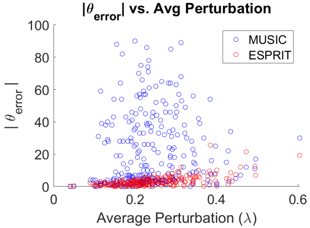

Figure: Single Source -15° with 50 Samples Per Average Perturbation Multiplier from 0.1λ in 0.1 increments for 1000 Snapshots for 0.1λ:0.1:0.5λ

Synthesizing Training & Validation Dataset

- Hierarchical Data Format Version 5 (HDF5) self-describing data storage method with groups, datasets, datastores, datatypes, and options for compression and other features
- Normalize HDF5 data [0,1] $\rightarrow$ convert to 3-channel images

$$\begin{bmatrix} 1.00+0.00j & -0.83+0.55j & 0.82+0.57j & -0.48-0.87j & 0.90-0.43j \\ -0.83-0.55j & 1.01+0.00j & -0.37-0.93j & -0.08+1.00j & -0.99-0.14j \\ 0.82-0.57j & -0.37+0.93j & 1.01+0.00j & -0.89-0.45j & 0.50-0.87j \\ -0.48+0.87j & -0.08-1.00j & -0.89+0.45j & 1.01+0.00j & -0.06+1.00j \\ 0.90+0.43j & -0.99+0.14j & 0.50+0.87j & -0.06-1.00j & 1.02+0.00j \end{bmatrix}$$

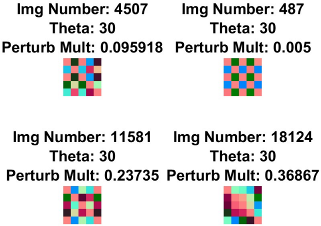

Figure: Example Images Produced using the Sample Covariance Matrix as the Red (Real), Green (Imaginary), and Blue (Phase) components

Original Regression Network

Deep Convolutional Neural Network (DCNN) regression network for DOA estimation under perturbations:

Table: Network Layers, Activations, and Learnables.
Total Learnables 413,313 Parameters.

Layer	Activations	Learnable Sizes	State Sizes
Image Input	5(S)x5(S)x3(C)x1(B)	-	-
Conv2D_3x3_32_1st	5(S)x5(S)x32(C)x1(B)	Weights 3x3x3x32 Bias 1x1x32	-
BatchNorm1	5(S)x5(S)x32(C)x1(B)	Offset 1x1x32 Scale 1x1x32	TrainedMean 1x1x32 TrainedVariance 1x1x32
ReLU1	5(S)x5(S)x32(C)x1(B)	-	-
Conv2D_1x1_64_2nd	5(S)x5(S)x64(C)x1(B)	Weights 1x1x32x64 Bias 1x1x64	-
BatchNorm2	5(S)x5(S)x64(C)x1(B)	Offset 1x1x64 Scale 1x1x64	TrainedMean 1x1x64 TrainedVariance 1x1x64
ReLU2	5(S)x5(S)x64(C)x1(B)	-	-
FullyConnected1_1600to256	256(C)x1(B)	Weights 256x1600 Bias 256x1	-
Dropout1	256(C)x1(B)	-	-
FullyConnected2_256to1	1(C)x1(B)	Weights 1x256 Bias 1x1	-

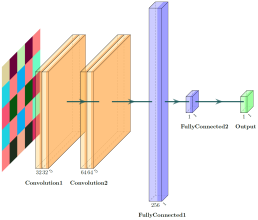

Figure: DCNN Layers

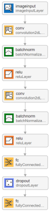

Figure: DCNN Layers Including Activations, Batch Norm, and Dropout

Regression Network Performance (1)

- Training the network 2.5min with 25,000 samples: 500 samples per 50 average perturbation values
- For various perturbation multipliers for a single angle the estimated angle from the DCNN was less than $|1^{\circ}|$ from the labeled angle.

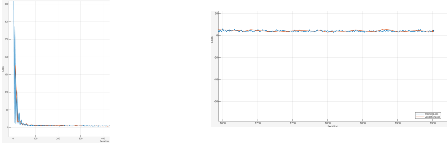

(a) Large MSE first 50 iterations

(b) Convergence Error Rate for the rest of the training process

Figure: Training Monitor with large initial training loss until iteration 60

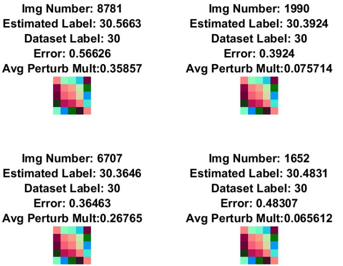

Figure: Testing samples with absolute value of angular error

Regression Network Performance (2)

Table: MUSIC and ESPRIT Estimation on Test Images

DOA Method	Image Number	Avg. Perturb Mult (λ)	Estimate	Absolute Error
MUSIC	11329	0.45959	73°	43°
ESPRIT	11329	0.45959	29.0444°	0.95555°
MUSIC	7395	0.29796	-46°	76°
ESPRIT	7395	0.29796	23.909°	6.091°
MUSIC	10112	0.40908	0°	30°
ESPRIT	10112	0.40908	-33.6229°	63.6229°
MUSIC	3770	0.15653	39°	9°
ESPRIT	3770	0.15653	25.2298°	4.7702°

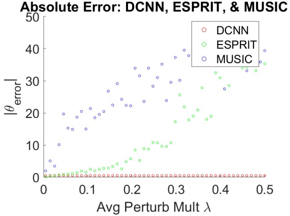

Figure: Comparison of Regression Absolute Error DCNN vs. MUSIC vs. & ESPRIT

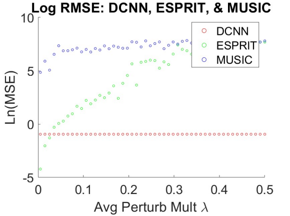

Figure: Comparison of Regression Log MSE DCNN vs. MUSIC vs. & ESPRIT

Visualization 32-3x3 Convolution Filters

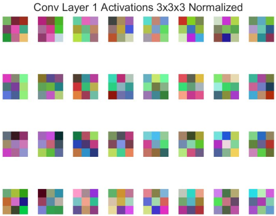

Figure: 3 Channeled 3x3 Filters Before ReLU

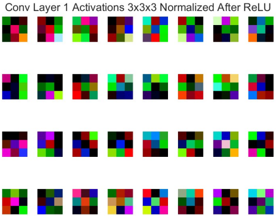

Figure: 3 Channeled 3x3 Filters After ReLU

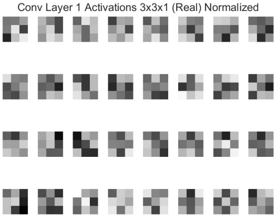

Figure: Single Channel Real Component Before ReLU

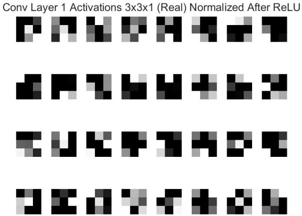

Figure: Single Channel Real Component Filters After ReLU

Variations on a Theme

- Altered original regression network using experiment manager in MATLAB for some parameters
- Convolution Filter Size, Fully Connected Layer Size, Network Topology, & Training Dataset

Table: Changing Network Topology for Single Source at 30°

Changes to Original Network	Elapsed Time (min:sec)	Training Loss	Validation Loss
1: Original Network	1:56	4.3198	4.9989
2: 128 Neurons Fully Connected Layer (FCL)	1:50	7.4965	7.1541
3: 2 More 32-3x3 Conv2D and 2 More 64-1x1 Conv2D Layers	2:41	4.2088	3.5664
4: Case 3 with 128 Neurons in FCL	6:05	6.3219	8.2020
5: Original Network with One Extra FCL 1st FCL 1024 Neurons & 2nd FCL 512 Neurons	6:22	4.5933	4.5607
6: Original Network Without Dropout Layer	5:57	0.0178	0.1827
7: Original Network Without Batch Normalization	3:43	7.7215	5.7125
8: Original Network with Single FCL from 1600 to 1 output (no dropout)	5:26	0.0248	0.2031
9: Swap 64-1x1 Conv2D with 32-3x3 Conv2D Layer from Original Network	5:40	4.0565	3.5487
10: 4 Total 1x1 Convolutions (Replaced 3x3 Convolution with This)	6:32	4.3543	13.1128

Table: Changing Training Dataset in Regression Network for Single Source at 30°

Dataset Channels	Elapsed Time (min:sec)	Training Loss	Validation Loss
Real,Imaginary,Phase	4:55	3.8489	3.7580
Real,Imaginary,Avg	5:30	4.1228	3.4121
Real,Imaginary,Absolute Value	5:22	3.8489	3.7580
Absolute Value,Phase,Avg	5:11	4.4550	6.6213

Feasibility Analysis for Classification Network and Expansion to $\pm 90^\circ$

- Classification Network requires one-hot encoding outputs & neuron size equal to number of classes & softmax on the output to assign probabilities to each class & categorical cross-entropy loss function
- Network was expanded for $\pm 90^\circ$ DOA case:
  * 2 layers 64-3x3 Conv2D
  * 2 layers 64-1x1 Conv2D
  * Dense: 1024-512-256-1

Table: Classification Network for [-90° , 90°]

Dataset Labeled DOA	Network Output DOA	DOA Estimation Error
63°	23°	40°
-37°	68°	-105°
13°	13°	0°
-14°	47°	-61°
17°	23°	-6°
-32°	-36°	4°
-72°	-83	11°
77°	78°	-1°
29°	-78°	107°
-79°	-83°	4°

Table of Contents

Summary

- Classical DOA methods are not reliable for element perturbations
- DOA Estimation is feasible for a single angle under large element perturbations using a simple regression Convolutional Neural Network (CNN)
- On average ESPRIT is fairly resilient to element position perturbations
- Grating lobes, snapshot number, and accessible features are limiting in achievable Field of View (FOV) for DOA estimation

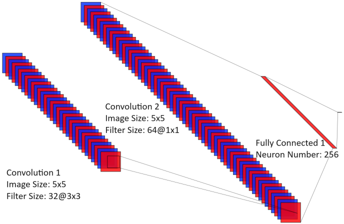

Figure: Representation of the Regression CNN Used

Future Work

- Application of the network topology to larger angular region, that is not excessive either $\pm\ 30^\circ$ or $\pm\ 60^\circ$.
- Collection of Real-World Signal Samples
- Source Number determination similar to previous approaches (simpler with classification networks)
- Evaluation & Literature Review of Grid-less approaches and methods that strive for covariance matrix reconstruction
- Deep & Convolutional Autoencoder and testing other topologoies (GAN, RNN, Transfer Learning)
- Determination of DOA under different received signals (QPSK, FSK, etc.)
- Coherent and Wideband signal source cases

References (1)

1. A. Forenza, D. J. Love, and R. W. Heath, "Simplified spatial correlation models for clustered mimo channels with different array configurations," IEEE Transactions on Vehicular Technology, vol. 56, no. 4, pp. 1924–1934, 2007.
2. D. Corman, "A comprehensive guide to active antennas, beamforming101," 7 2018. `https://www.rfglobalnet.com/doc/a-comprehensive-guide-to-activeantennas-or-beamforming-0001`.
3. Z.-M. Liu, C. Zhang, and P. S. Yu, "Direction-of-arrival estimation based on deep neural networks with robustness to array imperfections," IEEE Transactions on Antennas and Propagation, vol. 66, no. 12, pp. 7315–7327, 2018.
4. J. P. Merkofer, G. Revach, N. Shlezinger, T. Routtenberg, and R. J. G. van Sloun, "Da-music: Data-driven doa estimation via deep augmented music algorithm," IEEE Transactions on Vehicular Technology, vol. 73, no. 2, pp. 2771–2785, 2024.
5. P. K. Eranti and B. D. Barkana, "An overview of direction-of-arrival estimation methods using adaptive directional time-frequency distributions," Electronics, vol. 11, no. 9, 2022.

References (2)

6. G. Ajmera, “Decoding activation functions: Navigating the landscape for image segmentation,” 12 2023. https://medium.com/@girishajmera/decodingactivation-functions-navigating-the-landscape-for-image-segmentationf091e971e475.
7. I. Goodfellow, Y. Bengio, and A. Courville, Deep Learning. 2016.
8. “Cs231n convolutional neural network for visual recognition,” 2024. https://cs231n.github.io/neural-networks-2/.
9. Z. Dai, Y. He, V. Tran, N. Trigoni, and A. Markham, “Deepaoanet: Learning angle of arrival from software defined radios with deep neural networks,” IEEE Access, vol. 10, pp. 3164–3176, 2022.
10. A. M. Elbir, “Deepmusic: Multiple signal classification via deep learning,” IEEE Sensors Letters, vol. 4, no. 4, pp. 1–4, 2020.
11. D. H. Shmuel, J. P. Merkofer, G. Revach, R. J. G. van Sloun, and N. Shlezinger, “Deep root music algorithm for data-driven doa estimation,” in ICASSP 2023 - 2023 IEEE International Conference on Acoustics, Speech and Signal Processing (ICASSP), pp. 1–5, 2023.

Thank You!

Questions?

Supplemental content

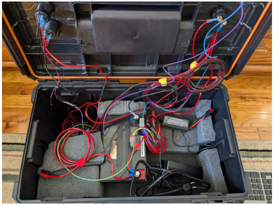

Figure: Battery Case Internals: 40Ah $LiFePo_4$ with charging ports

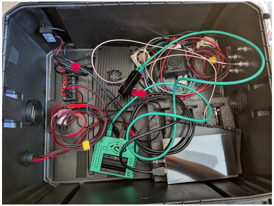

Figure: Kraken SDR Box with Jetson Nano, Anderson Power Distribution, Screen, and other equipment

Figure: External Battery Case

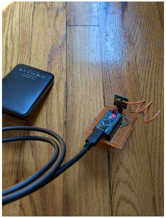

Figure: ASK Simple Transmitters from Arduino Nano & FS1000